

Distance Dependence of Electron Transfer in DNA: The Role of the Reorganization Energy and Free Energy

H. L. Tavernier and M. D. Fayer*

Department of Chemistry, Stanford University, Stanford, California 94305

Received: April 7, 2000; In Final Form: October 1, 2000

A model of the distance dependence of photoinduced donor–acceptor electron transfer in DNA is presented that includes the distance dependence of the solvent reorganization energy and free energy in the heterogeneous DNA environment. DNA is modeled as a low dielectric region that represents the base stack and two regions with more moderate dielectric properties that represent the DNA backbone. The DNA is surrounded by a high dielectric medium, which represents water. Model calculations show the importance of including the reorganization energy and the free energy change and illustrate the differences between the inhomogeneous model and homogeneous single dielectric constant calculations using standard Marcus theory. Calculations are performed for comparison to published experimental work (*Science* **1997**, 277, 673;¹ *J. Am. Chem. Soc.* **1992**, 114, 3656²). Fits to one set of data² permit the previously reported distance dependence to be separated into an electronic contribution and solvent reorganization energy and free energy contributions. For the other set of data,¹ inclusion of the solvent reorganization energy and free energy distance dependences in the analysis of the overall distance dependent data suggest that the Marcus form of the distance dependent rate constant including the Marcus reorganization energy is not consistent with the data.

I. Introduction

The distance dependence of electron transfer in DNA has been a topic of significant interest in recent years. Numerous experimental studies have been performed, resulting in reports of widely varying distance dependences of the electron transfer.^{1–14} Some of the experimental systems studied appear to undergo almost distance-independent electron transfer.^{4–10} Theories to explain this work include pair wise hopping mechanisms,¹⁵ wavelike electron transfer through a delocalized bridge system,¹⁶ and thermally activated pair wise transfer via base pairs.¹⁷ Some experimental work shows a distance dependence typical of superexchange or electron tunneling (Marcus-like) observed for inter- and intramolecular electron transfer in a wide variety of environments, including proteins, liquids, and micelles.^{1–3,11–14} It has recently been suggested that electron transfer in DNA may occur by different mechanisms depending on the energetics of a specific system.¹⁵

The focus of this paper is to examine the role played by the distance dependence of the reorganization energy and the free energy associated with electron transfer on the overall distance dependence of single-step electron transfer (Marcus-like transfer) in the heterogeneous DNA environment. Model calculations are presented to illustrate the nature of the effects, and the model is applied to examples of data reported in the literature.^{1,2} Previously, data have been analyzed primarily using a simple exponential distance-dependent rate, $k_e(r)$,^{1–3,11}

$$k_e(r) = Ae^{-\beta_e r_e} \quad (1)$$

where r_e is the edge-to-edge distance between the donor and acceptor molecules, A is a preexponential factor, and β_e characterizes the exponential distance dependence of the transfer.

Equation 1 can be useful to characterize the distance dependence approximately. However, some of the parameters that affect the rate of electron transfer have a distance dependence of their own. A true characterization of the distance dependence of the transfer must separate the falloff of the electronic coupling from the distance dependence of other factors affecting transfer.

This paper presents an approach in which a more detailed, Marcus form of the distance-dependent electron transfer rate constant is used to analyze previously published data on electron transfer in DNA. Because multistep electron-transfer processes also depend on free energies (ΔG) and reorganization energies (λ), properly including the heterogeneous environment and the correct distance dependences of these parameters is important for a full analysis of such problems. The inclusion of ΔG and λ in an inhomogeneous dielectric environment has already been applied to the case of electron transfer in micelles.¹⁸ The micelle environment can be separated into three dielectric regions: a low dielectric core, headgroup region with moderate dielectric properties, and water exterior. Distance-dependent λ and ΔG can be calculated analytically for electron transfer within this three-phase environment. In this paper, the same approach is used to calculate distance-dependent λ and ΔG for the case of electron transfer in DNA so that their effects can be separated from the distance dependence of the electronic coupling.

The DNA environment is modeled with four dielectric regions: a low dielectric region that represents the base stack, two regions with moderate dielectric properties representing the backbones of the double helix, and surrounding water. The continuous regions representing the DNA are modeled by a series of overlapping spheres, one positioned at each base or sugar–phosphate group location. The entire system is surrounded by water, creating a four-part dielectric environment. Although overlapping spheres are used in the numerical calculations, it is important to emphasize that regions are continuous with complex shapes consistent with the structure

* Corresponding author. E-mail: fayer@fayerlab.stanford.edu. Fax: (650) 723-4817.

of DNA. In all the cases presented, the distance dependence of electronic coupling is shallower than that calculated with a simpler, exponential rate (eq 1). While the model is an approximate representation of the problem of electron transfer in DNA, it is sufficiently detailed to illustrate the importance of factors that have long been considered in other contexts such as electron transfer between a donor and acceptor in liquid solution.^{18–22}

II. Theory

In 1956 Marcus developed an expression for the distance-dependent rate of electron transfer via electron tunneling.^{19,20,23} Since that time, his expression has been used to effectively describe electron transfer under a variety of conditions.^{24,25} The rate of electron transfer, $k(r)$, can be written

$$k(r) = \frac{2\pi}{\hbar} J_0^2 \exp[-\beta(r - r_0)] \frac{1}{\sqrt{4\pi\lambda(r)k_B T}} \times \exp\left[\frac{-(\Delta G(r) + \lambda(r))^2}{4\lambda(r)k_B T}\right] \quad (2)$$

where r is the distance between the centers of the donor and acceptor molecules and r_0 is the distance at which the donor and acceptor hard spheres are in contact. J_0 is the contact value of the donor/acceptor electronic coupling matrix element, and β characterizes the distance dependence of the coupling. The last exponential term is an activation energy. $\lambda(r)$ is the distance-dependent reorganization energy, and $\Delta G(r)$ is the distance-dependent free energy change of transfer. \hbar is Planck's constant over 2π , k_B is Boltzmann's constant, and T is temperature.

Duplex DNA can be viewed as a series of rows, each of which contains two sugar–phosphate backbone units and two nucleobases. Figure 1 shows a schematic of the model used in this paper, in which DNA is represented by rows containing four spheres. In the figure, spheres are nonoverlapping for clarity. However, in calculations the spheres interpenetrate, creating one helical ribbon that includes all the bases with two ribbons representing backbone chains on either side of the base stack. The outermost two ribbons represent the sugar–phosphate backbone, which has dielectric properties between those of hydrocarbon and water. The inner ribbon represents the nucleobases; it has a dielectric constant that is less than that of the sugar–phosphate backbone but greater than hydrocarbons. As in the Marcus theory, electron donors and acceptors are assumed to be conducting spheres. The appropriate size and location of each sphere must be determined for each specific system that is studied. Solvent reorganization energy and free energy of transfer for this model can be calculated using an approach developed previously and applied to electron transfer in micelles^{18,26} as long as the positions, sizes, and dielectric properties of ribbons are specified. In the numerical calculations, this is accomplished via the locations of the overlapping spheres.

The difference between the DNA (or micelle) problem and the Marcus description of electron transfer in solution is the heterogeneous nature of the medium in which the electron transfer is occurring. In the normal Marcus treatment, the donor and acceptor are spheres embedded in a homogeneous dielectric continuum. In the DNA problem, the donor and acceptor reside in a heterogeneous dielectric environment.

A. Reorganization Energy. Reorganization energy (λ) is the change in free energy required to move the reactant atoms to the product configuration and to move solvent molecules as if they were solvating the products, without actually transferring

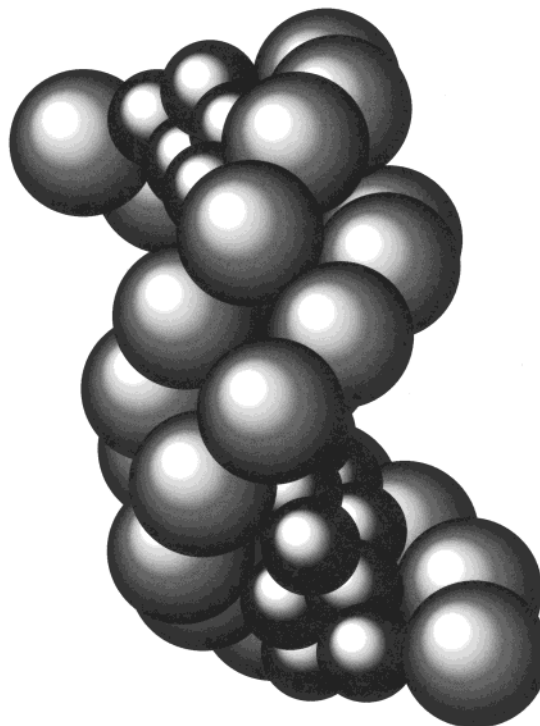


Figure 1. Schematic illustration of DNA used in the heterogeneous model for reorganization energy and free energy calculations. Each row contains four spheres; the two innermost spheres are small and represent a nucleobase pair while the two larger exterior spheres each represent a sugar–phosphate backbone unit. Three-dimensional coordinates of spheres were extracted from X-ray crystal structure data. In the calculations, the spheres overlap to define four distinct dielectric regions: a base stack ribbon, two backbone ribbons, and surrounding water. For clarity, spheres do not overlap in this figure.

the electron. It includes an inner-sphere (λ_i) portion and an outer-sphere or solvent portion (λ_o):²⁷

$$\lambda = \lambda_i + \lambda_o \quad (3)$$

Marcus developed an expression for λ_o for electron transfer in a dielectric continuum.^{19,20,23} This approach can be extended to heterogeneous media if all space can be divided up into a number of regions with different dielectric properties. In this case, solvent reorganization energy is given by

$$\lambda_o = \sum_q \frac{e^2 \alpha_q}{8\pi} \int_{v_q} (\mathbf{E}_D - \mathbf{E}_A)^2 dV \quad (4)$$

where q represents the four different dielectric regions, which together occupy all space excluding the donor and acceptor volumes. e is the charge of an electron. Optical and static dielectric constants of each region are included in the term $\alpha_q = \epsilon_{op,q}^{-1} - \epsilon_{st,q}^{-1}$. v_q is the volume of each region, q . $\mathbf{E}_{D/A}$ are the vectors of electric displacement determined by the total charge distribution on the donor/acceptor. Following the approach of Marcus,¹⁹ the electric induction is approximated by the electric field due to a given charge distribution in a vacuum,

$$\mathbf{E}_{D/A}(\mathbf{r}) = -\nabla|\mathbf{r} - \mathbf{r}_{D/A}|^{-1} \quad (5)$$

where $\mathbf{r}_{D/A}$ is the location of the center of the donor/acceptor sphere.

For the model of DNA shown in Figure 1, λ_o is calculated by first integrating over all space with the dielectric properties of the solvent, i.e., water. For each smaller region (a ribbon),

the contribution from the region is added to λ_o and the contribution from the solvent for that volume is subtracted from λ_o . λ_o can be rewritten more clearly

$$\lambda_o = \frac{e^2 \alpha_s}{8\pi} \int_{v_o - v_D - v_A} (\mathbf{E}_D - \mathbf{E}_A)^2 dV + \sum_{q \neq s} \frac{e^2 (\alpha_q - \alpha_s)}{8\pi} \int_{v_q} (\mathbf{E}_D - \mathbf{E}_A)^2 dV \quad (6)$$

where s represents the solvent surrounding the DNA. The first term in eq 6 is λ_o for a continuum solvent.

B. Free Energy. The free energy change of photoinduced electron transfer, $\Delta G(r)$, is another distance-dependent parameter that affects the distance-dependent electron-transfer rate constant. Determination of $\Delta G(r)$ requires knowledge of oxidation/reduction potentials of the donor/acceptor and calculation of the distance-dependent Coulombic interactions of the reactants and products. Often, redox potentials are known for donor/acceptor molecules in a bulk liquid, but not in the heterogeneous environment of a DNA duplex. The different local dielectric environments near the donor/acceptor molecules also affect Coulombic interactions. However, these factors can be calculated to determine the distance dependence of ΔG in the DNA duplex.

In general, $\Delta G(r)$ for photoinduced forward electron transfer can be written²⁸

$$\Delta G(r) = IP_D - EA_A - W_r + W_p - h\nu \quad (7)$$

where IP_D is the ionization potential of the donor, EA_A is the electron affinity of the acceptor, $W_{r/p}$ denote the total energy change to bring the reactants/products together in the DNA duplex at the given separation distance, h is Planck's constant, and ν is the frequency at which the donor's normalized absorption and fluorescence spectra cross.²⁴ Determination of these values for the heterogeneous DNA environment follows the method developed by Weller for calculating redox potentials in one bulk solvent when redox potentials are known in a solvent with different dielectric properties.²⁹ Following this method, ΔG in a DNA duplex can be calculated from oxidation/reduction potentials measured in bulk solution.

The ionization potential of the donor and the electron affinity of the acceptor can be written in terms of donor/acceptor oxidation/reduction potentials ($E^{\text{ox/red}}$) and solvation free energies as follows:

$$IP_D - EA_A = (E_D^{\text{ox}} - E_A^{\text{red}})_B + \left(1 - \frac{1}{\epsilon_B}\right)(S_p - S_r) \quad (8)$$

where B denotes measurements made in a bulk liquid with static dielectric constant ϵ_B and $S_{r/p}$ is the electrical work required to create infinitely separated, charged reactant/product spheres in a vacuum:

$$S_{r/p} = \frac{e^2}{8\pi} (q_D^2 \int_{\infty - v_D} \mathbf{E}_D^2 dV + q_A^2 \int_{\infty - v_A} \mathbf{E}_A^2 dV) = \frac{e^2}{2} \left(\frac{q_D^2}{a_D} + \frac{q_A^2}{a_A} \right) \quad (9)$$

q_D and q_A are the charges on the donor/acceptor in units of e . Reactant charges should be used for calculation of S_r and product charges for S_p . $IP_D - EA_A$ is a relation of gas-phase properties, so eq 8 is valid for calculating ΔG of electron transfer in a bulk liquid or in a heterogeneous DNA environment. When

redox potentials are known for reactants already incorporated in the DNA duplex, the entirety of eq 8 must be evaluated for that environment:

$$IP_D - EA_A = (E_D^{\text{ox}} - E_A^{\text{red}})_{\text{DNA}} + \left(1 - \frac{1}{\epsilon_s}\right)(S_p - S_r) - \sum_{q \neq s} \left(\frac{1}{\epsilon_q} - \frac{1}{\epsilon_s}\right) \frac{e^2}{8\pi} \int_{v_q} ((q_{Dp}^2 - q_{Dr}^2) \mathbf{E}_D^2 + (q_{Ap}^2 - q_{Ar}^2) \mathbf{E}_A^2) dV \quad (10)$$

where \mathbf{E}_D and \mathbf{E}_A are given by eq 5 and ϵ_q are static dielectric constants. Equation 10 is valid for the case in which all space, except donor/acceptor volumes, is occupied by dielectric regions q , and region $q = s$ is the solvent surrounding all other regions.

$W_{r/p}$ terms incorporate both solvation energies and Coulomb interactions of the ions. $W_{r/p}$ can be written similarly to eq 6 for the case in which all space outside the conducting donor/acceptor spheres is occupied by dielectric regions q , including the surrounding solvent, s :

$$W_{r/p} = \frac{e^2}{8\pi \epsilon_s} \int_{\infty - v_D - v_A} (q_D \mathbf{E}_D + q_A \mathbf{E}_A)^2 dV + \sum_{q \neq s} \frac{e^2}{8\pi} \left(\frac{1}{\epsilon_q} - \frac{1}{\epsilon_s}\right) \int_{v_q} (q_D \mathbf{E}_D + q_A \mathbf{E}_A)^2 dV - S_{r/p} \quad (11)$$

Reactant and product charges are used for W_r and W_p , respectively. The first term in eq 11 is $W_{r/p}$ for a continuum solvent.

C. Details of the Calculations. Rate constants were calculated for the four-region dielectric model of DNA. Boundaries of the base stack and two backbone ribbon regions were defined as the boundaries of collections of overlapping spheres. The spheres, shown nonoverlapping for clarity in Figure 1, were located at coordinates obtained from the Protein Data Bank web page (www.rcsb.org/pdb). We used coordinate set 102D,³⁰ which is a double helical DNA strand consisting of 12 base pairs and the associated backbone atoms. In our calculations, one sphere is used to represent each base/backbone unit. The atomic coordinates can be quickly converted to our spherical model by selecting a central atom of each base/backbone unit to be the center of its representative sphere. For sugar-phosphate backbone units, the coordinates of the C1 atom were used. For spheres representing nucleobases, the atomic coordinates of C6, N3, C6, and N3 atoms were used for adenine, thymine, guanine, and cytosine, respectively. Using these coordinates, the average center-to-center distances between a base and its neighboring bases is 3.73 Å. The bases are very evenly spaced, and the distance between a base and its conjugate is essentially the same as the distance between neighboring bases on the same strand. In all our calculations, intermolecular electron-transfer distances are multiples of 3.73 Å, depending on the number of intervening base pairs. This value is slightly larger than the literature values cited for row height (3.4–3.5 Å)^{1,2,12} because it includes distance due to rotation of the layers to form the double helix. The center-to-center distance from a base sphere to its neighboring backbone sphere in the same row is 4.30 Å. The average distance between neighboring backbone spheres in the same strand is 4.96 Å. These values are very consistent for the entire set of duplex coordinates used. The intrastrand base-base distance is different from the intrastrand backbone-backbone distance due to the helical nature of the duplex.

From a space-filling molecular model of duplex DNA, in which each atom is accounted for, it is clear that there is not a

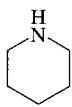
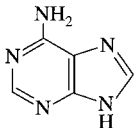
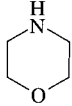
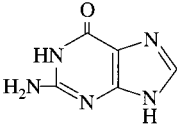
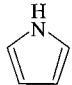
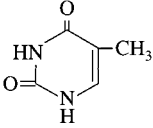
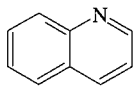
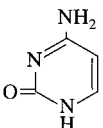
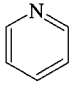
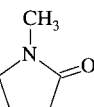
Molecule	Structure	ϵ_{st}	
Piperidine		5.8	Adenine 
Morpholine		7.4	Guanine 
Pyrrole		8.1	Thymine 
Quinoline		9.0	Cytosine 
Pyridine		12.4	
1-Methyl-2-pyrrolidinone		32.0	

Figure 2. Structures of nucleobases and some similar molecules along with the static dielectric constants, ϵ_{st} , of the molecules as pure liquids.⁴⁰

substantial amount of room left for solvent within the base stack. Accordingly, our calculations have been performed for the case in which sphere radii are large enough that they overlap to create more realistically continuous volumes. The set of base spheres creates a continuous volume that is assigned nonpolar dielectric properties. The backbone spheres create two continuous volumes, one on either side of the base stack. Regions in which base/backbone spheres overlap are assigned the dielectric properties of base spheres. This model is capable of illustrating the influence of the heterogeneous nature of DNA on single step, Marcus-like, electron transfer.

Base and backbone sphere radii were 2.35 and 3.09 Å, respectively. These are 25% larger than if the spheres were in contact but not overlapping. This increase falls within the range of atomic radii increases from covalent to van der Waals radii, which is 20% for carbon and 30–40% for halogens. As in the standard Marcus theory, donor/acceptor molecules are assumed to be conducting spheres, and integration is not performed over areas in which donor/acceptor spheres overlap other spheres.

Although it is often assumed that nucleobases have low dielectric constants (ϵ_{st} 2–4),³¹ similar molecules in bulk liquid have significantly higher dielectric constants. Figure 2 shows the structures of the nucleobases along with a number of similar, nitrogen-containing molecules and their bulk dielectric constants. The bases are most similar to molecules toward the bottom of the figure, which have moderate dielectric constants. Therefore, the region representing the base stack in the duplex DNA is taken to have optical and static dielectric constants of pyridine, $\epsilon_{op} = 2.27$ and $\epsilon_{st} = 12.4$. The sugar–phosphate backbone regions are assigned characteristics between those of pyridine and water, with $\epsilon_{op} = 1.90$ and $\epsilon_{st} = 20.0$. These regions are surrounded by a solvent with $\epsilon_{op} = 1.77$ and $\epsilon_{st} = 78.3$, the dielectric constants of water.

There are two issues associated with the assignments of dielectric constants. Because dielectric constants are continuum

properties, can they be assigned to small volumes? Propylene glycol in 2.5–7.5 nm pores has a fairly polar static dielectric constant, although it is less than that of bulk propylene glycol.³² Thus, small volumes of individual molecules can have bulklike dielectric properties although they are not the same as the bulk liquid. The second issue is assigning dielectric constants of freely moving bulk liquids to bases that are bound to the backbone and hydrogen-bonded to each other. However, calculations of the effective dielectric constant between atoms in adjacent adenines in B-DNA yield $\epsilon_{st} = 5–18$.³³ In addition, several theoretical studies of proteins have shown that amino acids with polar side groups can give the overall protein significantly polar character despite their restricted motion. Although the interior of the proteins are found to have $\epsilon_{st} = 2–3$, when the more polar amino acids on the exterior of the protein are included, the entire protein exhibits an effective $\epsilon_{st} = 15–25$.^{34,35} Therefore, as an initial model, it is useful and reasonably realistic to assign dielectric constants to the ribbons that are used to model DNA.

For bridged systems like DNA, λ_i can be determined by the donor/acceptor molecules independent of the length of intervening bridge.³⁶ An organic donor/acceptor pair typically has a λ_i of 0.06–0.4 eV.^{37–39} For the examples used in this paper, 0.4 eV $\ll \lambda_o$. As a result, λ_i affects the magnitude of $k(r)$ but has virtually no effect on the distance dependence of $k(r)$ (<2% change in slope). Consequently, λ_i is neglected in all of our calculations, leaving $\lambda = \lambda_o$.

In all calculations, the parameters given above were used unless otherwise specified. Rate calculations assumed the Marcus distance-dependent rate in eq 2. $\lambda(r)$ was calculated using eq 6, and $\Delta G(r)$ was calculated using eqs 7–9 and 11. Integrations in eq 6–11 were performed numerically.

D. Sensitivity to Parameters. Calculations were performed to check the sensitivity of the rate constant to exact radii, dielectric constants, coordinate sets, and proximity of the donor/acceptor to the end of the DNA duplex. Unless otherwise specified, the donor/acceptor radius is 1.87 Å, which corresponds to half the distance between neighboring bases. The acceptor replaced a base at the fourth row from the end of the duplex. The donor replaced a base farther from the end on the same strand, with 0–4 bases intervening. Donor/acceptor charges were 0, 0 \rightarrow 1, -1 for charge separation and 0, 1 \rightarrow 1, 0 for charge shift; $(E_D^{ox} - E_A^{red})_{\epsilon_{st} = 37} = 2.65$ eV; $h\nu = 3.35$ eV; $J_o = 100$ cm⁻¹; and $\beta = 1$ Å⁻¹.

Figure 3 shows the effect of dielectric constant on the heterogeneous calculations. $\ln(k)$ vs r is shown for both charge separation and charge shift. Calculations are shown for different combinations of dielectric constants for base stack ($\epsilon_{op} = 2.27$, $\epsilon_{st} = 4, 6, 12$) and backbone regions ($\epsilon_{op} = 1.9$, $\epsilon_{st} = 10, 20, 40$). It is important to note that while we will refer to the slope of $\ln(k)$, the curves are not straight lines. This is particularly noticeable in comparing the first point to the rest. The distance dependence has a curvature that becomes less pronounced at longer distance. Slopes of all the $\ln(k)$ plots were compared for 2 cases: including the first point, and not including the first point. Results were similar in both cases. The slope of $\ln(k)$ vs r was ~ -2.0 Å⁻¹ if all of the points were included, and ~ -1.5 Å⁻¹ if the first point was ignored. Both of these values are significantly different from the -1 that would be expected from a purely exponential rate with $\beta = 1$ Å⁻¹. On average, charge separation and charge shift have approximately the same distance dependence. For charge separation (Figure 3A), there is less than 6% change in the slope for this range of dielectric constants. Charge shift (Figure 3B), shows the opposite trend:

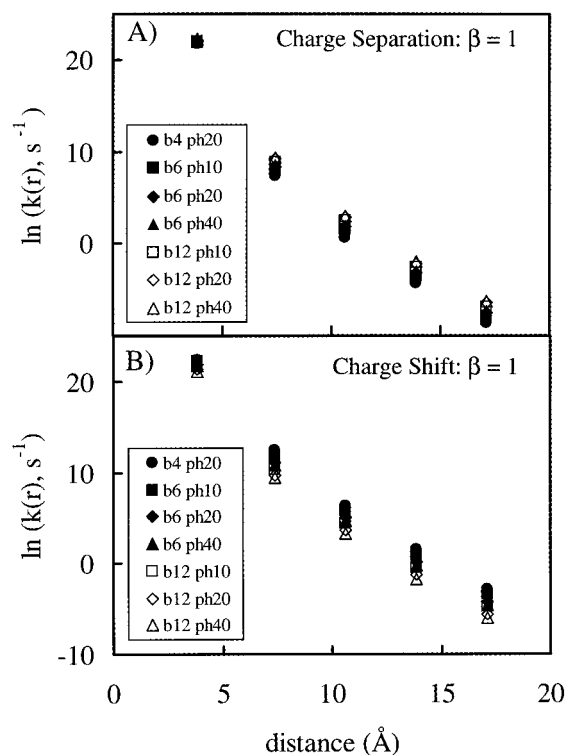


Figure 3. Natural log of the rate constant vs distance for electron transfer in a heterogeneous DNA model with a variety of nucleobase and backbone dielectric properties. The legend lists static dielectric constants of base (b) and sugar–phosphate backbone (ph) regions used in each calculation. (A) shows the case of charge separation ($D + A \rightarrow D^+ + A^-$). (B) shows the case of charge shift ($D + A^+ \rightarrow D^+ + A$). The rates are not highly dependent on the dielectric constants within a reasonable range.

|slope| increases as base or backbone dielectric constant increases. There is less than 8% difference in slope in all the different dielectric combinations for charge shift. However, for both charge shift and charge separation, the intercept of a line fit to $\ln(k)$ is dependent on dielectric constant and can increase/decrease by up to 2 units when the lowest dielectric constants are used. Slopes of calculations are not highly sensitive to exact dielectric constants within a physically reasonable range. On the other hand, dielectric constants must be chosen carefully if the magnitude of the rate constant is to be evaluated properly.

In addition, the following changes were compared: donor/acceptor radii of both 1.87 Å and both 2.35 Å, changing the free energy by making $h\nu = 2.95$ eV, acceptor placed at 1st, 2nd, and 4th rows, and an alternate coordinate set using C4 rather than N3 for thymine and cytosine. All of the parameter changes outlined in this paragraph yield slope changes of <5% for both charge shift and charge separation, when slopes are calculated all with or all without the 1st point. Intercepts of the lines fit to $\ln(k)$ vs r can increase/decrease by up to 1 unit for different coordinates or donor/acceptor locations, and up to 8 units for different donor/acceptor radii. Although intercepts are highly sensitive to donor/acceptor radii, the overall calculations are not highly sensitive to changes in other structural parameters of the model within the range of physically feasible parameters.

Finally, calculations were performed for base/backbone sphere sizes of 1.87 and 2.45 Å, respectively, which correspond to spheres that touch but do not overlap. The advantage of this size choice is that when the spheres comprising the DNA strand do not intersect each other or with the donor/acceptor spheres, λ and ΔG can be calculated analytically (see Appendix A). The result is a slope change of <4% for charge shift and charge

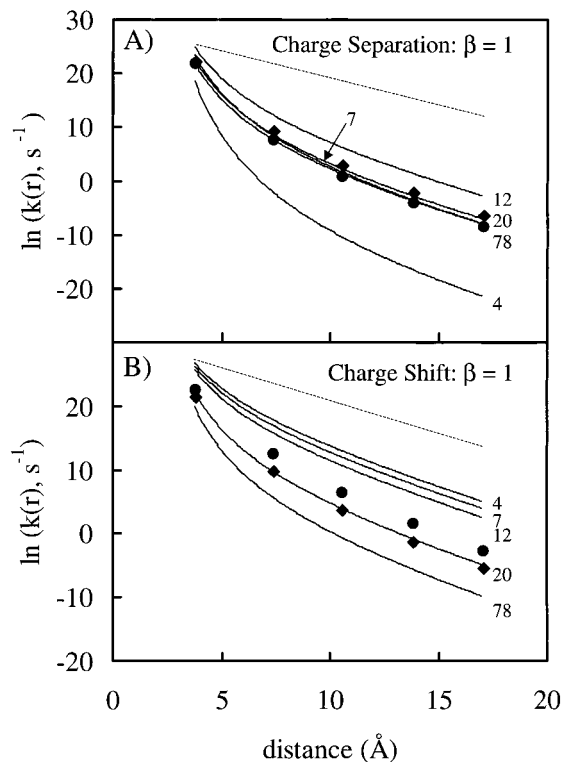


Figure 4. Natural log of the rate constant vs distance for electron transfer with $\beta = 1 \text{ \AA}^{-1}$. Solid lines are calculated for dielectric continua with static dielectric constants designated to the right. Calculations performed for heterogeneous DNA model are represented by circles (base $\epsilon_{st} = 4$, backbone $\epsilon_{st} = 20$), and diamonds (base $\epsilon_{st} = 12$, backbone $\epsilon_{st} = 20$ and 40 (indistinguishable)). The dashed line with slope = -1 represents a simple exponential rate with $\beta_e = 1 \text{ \AA}^{-1}$ in which the distance dependence of solvent reorganization energy and free energy are ignored. (A) Charge separation ($D + A \rightarrow D^+ + A^-$). (B) Charge shift ($D + A^+ \rightarrow D^+ + A$).

separation. However, the intercept can increase/decrease by up to 2 units. If only the slope is important, the analytical approach with smaller base/backbone spheres is a suitable, simpler first approximation.

III. Results and Discussion

A. Comparison to Continuum Rates. Figure 4 compares electron-transfer rate vs distance in dielectric continua with a variety of dielectric constants and in the heterogeneous multi-sphere DNA model. The cases of charge separation ($D + A \rightarrow D^+ + A^-$) and charge shift ($D + A^+ \rightarrow D^+ + A$) are shown in Figure 4A,B, respectively. Dielectric continuum curves shown in the figures were calculated with dielectric constants of ethyl ether ($\epsilon_{op} = 1.82$, $\epsilon_{st} = 4.34$), morpholine ($\epsilon_{op} = 2.12$, $\epsilon_{st} = 7.42$), pyridine ($\epsilon_{op} = 2.27$, $\epsilon_{st} = 12.4$), propanol ($\epsilon_{op} = 1.9$, $\epsilon_{st} = 20$), and water ($\epsilon_{op} = 1.77$, $\epsilon_{st} = 78.3$).⁴⁰ For the DNA calculations, the acceptor replaces a base at the 4th row from the end of the duplex, and the donor replaces another base on the same strand, at various positions further from the end of the duplex. Three sets of base/backbone dielectric parameters are shown for comparison to continuum calculations: (1) base $\epsilon_{op} = 2.27$, $\epsilon_{st} = 4.0$, backbone $\epsilon_{op} = 1.9$, $\epsilon_{st} = 20.0$, (2) same as (1) except base $\epsilon_{st} = 12.4$, and (3) same as (2) except backbone $\epsilon_{st} = 40.0$. All rate constants are calculated using the Marcus distance-dependent rate in eq 2, with $J_0 = 100 \text{ cm}^{-1}$ and $\beta = 1 \text{ \AA}^{-1}$. $\lambda(r)$ is calculated using eq 6 for both the continuum and DNA rates. In addition, $\Delta G(r)$ is calculated using eqs 7–9 and 11, with donor/acceptor radii = 1.87 Å, ($E_D^{ox} -$

$E_{\text{A}}^{\text{red}})_{\text{B}} = 2.65$ eV, $\epsilon_{\text{B}} = 37$, and donor photoexcitation energy $h\nu = 3.35$ eV for both continuum and DNA cases. Equations for the heterogeneous model collapse to continuum equations when all spheres are given the same dielectric constants. Performing the full calculation of $\Delta G(r)$ for the continuum rates ensures that redox potentials are corrected for dielectric constant.

In the charge separation calculation (Figure 4A) for the choice of parameters shown, as the continuum dielectric constant is made smaller ($78 \rightarrow 20 \rightarrow 12$), electron transfer becomes faster and falls off more slowly with distance. Further decrease in the dielectric constant ($12 \rightarrow 7 \rightarrow 4$) reverses this trend, and the electron transfer becomes slower and falls off more steeply with distance. For charge shift (Figure 4B), there is a monotonic increase in the rate of electron transfer and a decrease in the fall off with distance as the dielectric constant is decreased. (Note that for either charge separation or charge shift, if the dielectric constant is made small enough, e.g., benzene ($\epsilon_{\text{op}} = 2.24$, $\epsilon_{\text{st}} = 2.28$), electron transfer is very slow and the curves are off the bottom of the graphs.)

The distance dependence calculations for the DNA model have electron transfer magnitudes and distance dependences that are similar to some of the curves calculated using the Marcus theory for a dielectric continuum. Given the similarities in the shapes of the curves it might be possible to use a continuum model for electron transfer in DNA, but the choice of the continuum dielectric constant is not obvious. This is particularly true for the case of charge separation. Static dielectric constants of 7, 20, and 78 all agree well with the heterogeneous DNA calculations, while values of 4 and 12 do not agree. We have used a dielectric constant of 20 for the sugar-phosphate backbone regions. The continuum calculations for both charge shift and charge separation using 20 as the dielectric constant agree well with the heterogeneous DNA calculations. However, this is for a particular placement of the donor and acceptor in the DNA and using the particular choices of the other parameters. This result is not true for all sets of parameters. An effective dielectric constant of 20 is plausible for a case in which molecules are surrounded in part by water, in part by a hydrocarbon-like region, and in part by regions of moderate polarity (see Figure 1). For example, it has been shown that $\epsilon_{\text{st, effective}} = 20$ in the minor groove of DNA.⁴¹

Also included in Figure 4A,B are straight lines which represent a simple exponential rate, as in eq 1, with slope = -1 , i.e., $\beta_{\text{e}} = 1 \text{ \AA}^{-1}$. This represents the case in which the distance dependences of the reorganization energy and free energy are ignored. Both the Marcus continuum and heterogeneous DNA electron-transfer rates were calculated with $\beta = 1 \text{ \AA}^{-1}$. Comparing the dashed line to the other calculated curves in the figure shows how significantly the distance dependence of λ and ΔG affect the overall rate constant. If the distance dependences of λ and ΔG were insignificant, the plot of $\ln(k)$ vs r would be linear with slope -1 for both continuum and DNA rates. Comparisons of the distance-dependent rates to the dashed line of slope -1 show that λ and ΔG play a significant role in the electron transfer. Fits to the calculated DNA rate (diamonds, base $\epsilon_{\text{st}} = 12$, backbone $\epsilon_{\text{st}} = 20$) assuming the simple exponential model in eq 1 would determine that $\beta_{\text{e}} = 2.1 \text{ \AA}^{-1}$, when, in fact, electronic coupling falls off with a factor $\beta = 1.0 \text{ \AA}^{-1}$. The rest of the distance dependence is due to λ and ΔG . Figure 4B shows $\ln(k)$ vs distance for charge shift continuum and DNA rates. Again, a line fit to the calculated $\ln(k)$ vs r for the heterogeneous DNA model yields a slope of -2.0 \AA^{-1} , significantly greater than the electronic coupling contribution, $\beta = 1.0 \text{ \AA}^{-1}$, used in the calculation. Simple

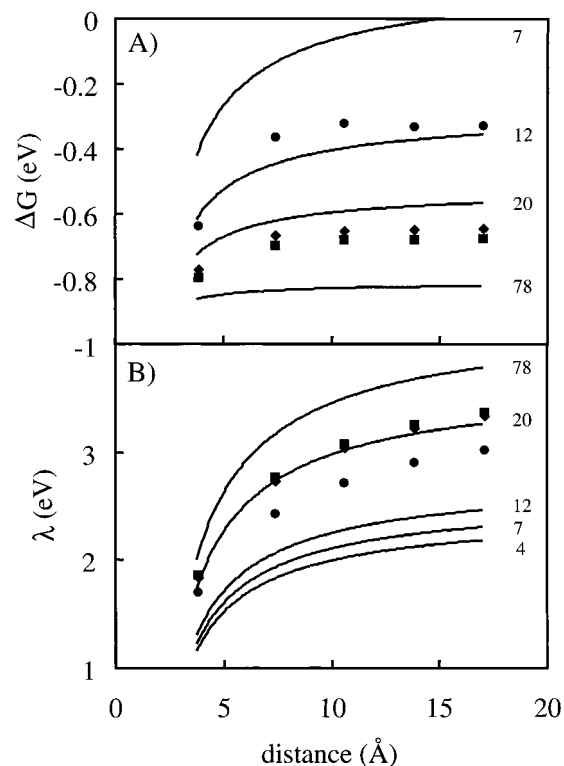


Figure 5. (A) Free energy change for charge separation electron transfer vs distance. (B) Solvent reorganization energy vs distance. For both plots, continuum calculations are represented by solid lines with static dielectric constants designated to the right. Calculations performed for heterogeneous DNA model are represented by circles (base $\epsilon_{\text{st}} = 4$, backbone $\epsilon_{\text{st}} = 20$), diamonds (base $\epsilon_{\text{st}} = 12$, backbone $\epsilon_{\text{st}} = 20$) and squares (base $\epsilon_{\text{st}} = 12$, backbone $\epsilon_{\text{st}} = 40$).

exponential fits to charge separation electron-transfer data could lead to determination of a β value that is incorrect by more than a factor of 2. It is also important to note that the result of a simple exponential fit is larger than the true electronic beta.

Heterogeneous DNA calculations in Figure 4 look somewhat similar for all three sets of dielectric constants used. However, this does not mean that all the factors contributing to the rate constant are similar for all sets of dielectric constants. In addition to the distance-dependent electronic coupling, the rate constant includes a distance-dependent activation energy that is dependent on $\Delta G(r)$ and $\lambda(r)$. Figure 5 shows calculated $\Delta G(r)$ and $\lambda(r)$ for continua and for all three sets of dielectric parameters used in the DNA calculations in Figure 4. $\Delta G(r)$ values (Figure 5A) are only shown for the case of charge separation because there is no distance dependence for charge shift when donor/acceptor are the same size and in similar environments. $\lambda(r)$ values (Figure 5B) are identical for charge shift and charge separation reactions. Diamonds and squares, representing base $\epsilon_{\text{st}} = 12$, backbone $\epsilon_{\text{st}} = 20$ and 40, are very similar to each other for $k(r)$, $\Delta G(r)$ and $\lambda(r)$ values. However, circles, representing base $\epsilon_{\text{st}} = 4$, backbone $\epsilon_{\text{st}} = 20$, have very different distance dependences and values of ΔG and λ . Values of ΔG and λ as a function of distance are much more sensitive to base/backbone dielectrics than are the overall rate constants because ΔG and λ are summed to calculate activation energy, and some of their differences cancel when the rate constant is calculated.

The results of the model calculations clearly show the importance of including the distance dependence of the reorganization energy and the free energy in a heterogeneous environment when trying to understand single step electron-transfer processes in DNA. Imagine that the model calculations

TABLE 1

	β_e (\AA^{-1}) ^a	β (\AA^{-1}) ^b
Brun and Harriman, ² EB ⁺ DAP ²⁺	0.91	0.61
Brun and Harriman, ² AOH ⁺ DAP ²⁺	0.86	0.61
Lewis et al., ¹ guanine stilbene	0.64	N/A

^a Beta for fit to exponential rate, eq 1. ^b Beta for fit to Marcus rate for heterogeneous DNA model, eq 2.

(the diamonds in Figure 4A,B) are experimental data. If a simple exponential distance dependence (eq 1) is used to describe the data, a fit will yield the parameter, β_e , but its meaning is unclear. It characterizes the distance dependence of the overall transfer, but it does not separate the distance dependence of electronic interaction from the other distance-dependent factors that influence the rate of electron transfer. If the Marcus approach for a homogeneous medium is used (eq 2), a fit can be made to both J_0 and β , but it is unclear which value of the dielectric constant should be used in the calculation of the reorganization energy or the free energy. The values of J_0 and β that will emerge are dependent on the choice of the "homogeneous" dielectric constant, and can yield errors of up to 50% in determination of β . The heterogeneous dielectric model that has been presented contains the important features of the problem that are necessary for a proper analysis of experimental data.

B. Comparison to Brun-Harriman Results. In 1992, Brun and Harriman published data for photoinduced electron transfer between intercalated molecules in duplex DNA.² The electron acceptor was *N,N'*-dimethyl-2,7-diazapyrenium dichloride (DAP²⁺). Two photoexcited donors were used: ethidium bromide (EB⁺) and acridine orange (AOH⁺). Rate vs distance was plotted on a semilog plot and fit to a straight line, using eq 1. The β_e obtained for these exponential fits are listed in Table 1.

Our calculations for comparison to these data included the following details. Radii of the DNA spheres are chosen in accordance with the space-filling model. Radii of DAP²⁺, EB⁺, and AOH⁺ used are 3.25, 3.64, and 3.47 \AA , respectively. These were calculated roughly, assuming 4.5 \AA^3 per atom and converting the volume to a sphere. The most accurate way to model this system would be to have coordinates from crystal structure of the DNA with intercalated molecules. Lacking these coordinates, the intercalated molecules were instead placed in specific rows by taking the average coordinates of the two bases in that row. Though this does not take into account disruptions in the stacking due to intercalation, it is a good first approximation of the complex heterogeneous local environment. The acceptor was placed at the third row from the end of the duplex, and the donor at rows 7–9. λ was calculated using eq 6. For this particular case of charge shift, all the $S_{r/p}$ and $W_{r/p}$ terms in eqs 7 and 9–11 cancel, leaving $\Delta G(r) = (E_D^{\text{ox}} - E_A^{\text{red}})_{\text{DNA}} - hv = -0.259$ and -0.675 eV for EB⁺ and AOH⁺, respectively.²

Figure 6 shows experimental data obtained by Brun and Harriman as well as calculations using the DNA sphere model. Parts A and B of the figure show data for acceptors EB⁺ and AOH⁺, respectively. Exponential fits to the data yield $\beta_e = 0.91$ and 0.86 \AA^{-1} for EB⁺ and AOH⁺, respectively. However, the best fit to the data using the heterogeneous DNA model uses $\beta = 0.61 \text{ \AA}^{-1}$ for both EB⁺ and AOH⁺. This result is in line with studies of electron transfer in ruthenium trisbipyridyl-viologen molecules, in which the distance dependence of the activation energy contributed $0.2\text{--}0.4 \text{ \AA}^{-1}$ of the rate constant's distance dependence.⁴² Thus, β_e is not a very good approximation to the distance dependence of the electronic coupling. Including the distance dependence of λ and ΔG indicates that the electronic coupling between the donor and acceptor molecules falls off 45% less steeply with distance than was previously estimated.

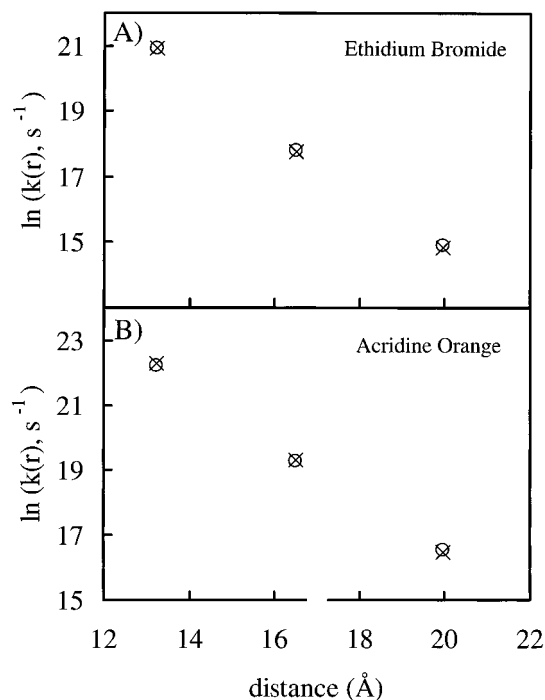


Figure 6. Natural log of the rate constant vs distance for both experimental data and calculations of electron transfer in DNA. Exact intermolecular center-to-center distances from X-ray crystal structure coordinates are used for distances for both experimental and calculated data. (A) Electron transfer from intercalated ethidium bromide to intercalated *N,N'*-Dimethyl-2,7-diazapyrenium dichloride. Circles represent data taken by Brun and Harriman, which can be fit to $\beta_e = 0.91 \text{ \AA}^{-1}$ using a simple exponential rate constant.² Crosses represent calculation using the heterogeneous DNA model with $\beta = 0.61 \text{ \AA}^{-1}$. (B) Electron transfer from intercalated acridine orange to intercalated *N,N'*-dimethyl-2,7-diazapyrenium dichloride. Circles represent data taken by Brun and Harriman, which can be fit to $\beta_e = 0.86 \text{ \AA}^{-1}$ using a simple exponential rate constant.² Crosses represent calculation using the heterogeneous DNA model with $\beta = 0.61 \text{ \AA}^{-1}$.

J_0 values of 2800 and 400 cm^{-1} were obtained for EB⁺ and AOH⁺, respectively. The differences in J_0 are due to the significant differences in ΔG of the two reactions. There could be significant error in these values because donor/acceptor radii and DNA base/backbone dielectric constants are not known precisely. Nonetheless, these values are physically reasonable.

It should be noted that Harriman recently reported attempts to measure λ in the EB⁺/DAP²⁺/DNA system.⁴³ Values of λ near 0.5 eV were obtained from the data analysis. The analysis, which depends on temperature-dependent experiments, assumes temperature-independent values of λ and ΔG . However, λ and ΔG are temperature dependent.⁴⁴ Thus, the experimental determination of λ is called into question. Our calculations predict λ values near 1.1 eV. Furthermore, Harriman's reorganization energy values decrease with increasing distance, unlike our calculations. Harriman attributed the decrease to increased disruption of the base stacking for smaller separation intercalations, so the dielectric environment is more polar for shorter distances. Even if polarity varied somewhat with donor/acceptor distance, the only way to calculate a value of λ near 0.5 eV by varying dielectric constants and radii was to use $\epsilon_{\text{op}} = 1.9$ and $\epsilon_{\text{st}} = 3$ for all DNA spheres and solvent. However, this seems unlikely since in the minor groove of DNA it was determined that $\epsilon_{\text{st, effective}} = 20$.⁴¹ The requirement of nearly-hydrocarbon environment casts further doubt on the validity of Harriman's data analysis.

C. Comparison to Lewis et al. Results. In 1997, Lewis et al. published data for photoinduced electron transfer from

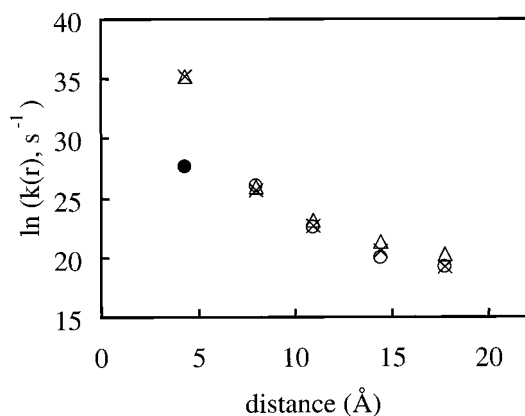


Figure 7. Natural log of the rate constant vs distance for electron transfer from guanine to a stilbenedicarboxamide bridge in DNA. Circles represent data taken by Lewis et al.¹ with distances calculated from exact intermolecular coordinates. The solid circle is a lower limit of the rate at that distance.⁴⁵ The data can be fit with $\beta_e = 0.64 \text{ \AA}^{-1}$ using a simple exponential rate constant. Crosses represent calculations using the heterogeneous DNA model with $\beta = 0.08 \text{ \AA}^{-1}$. Triangles represent the contribution from activation energy ($\beta = 0.0 \text{ \AA}^{-1}$), i.e., the contribution to the distance dependence from the reorganization energy and the free energy change. Similar calculated results are obtained using a continuum model (single dielectric constant) that includes the reorganization energy and the free energy change.

guanine to a stilbenedicarboxamide bridge incorporated into a DNA hairpin.¹ The hairpin was prepared with seven bases on each strand. A stilbenedicarboxamide bridge connected the two strands at one end. Six different types of hairpins were prepared. One type was composed of only AT pairs, and each of the other hairpins contained one CG pair, separated from the stilbene by 0–4 AT pairs. The shape of the resulting hairpins are believed to closely resemble a well-stacked B-form double helix, with the stilbene approximately 0.5 \AA farther from the first base pair than would be expected if it stacked exactly like a base pair.^{1,45} The rate of electron transfer from guanine to photoexcited stilbene was measured for each donor/acceptor separation distance separately, and the experimental results are plotted along with a theoretical calculation in Figure 7. The β_e value determined by Lewis et al. using exponential fits is listed in Table 1.

The theoretical rate vs distance plotted in Figure 7 was calculated using the four-region DNA model. Only the first eight rows of sphere coordinates were used. The stilbenedicarboxamide bridge was modeled by a sphere centered between the bases in the first row but 0.5 \AA farther away from the 2nd row, along the axis of the DNA. A radius of 2.47 \AA was used, so that the acceptor was in contact with the donor in the closest position. The donor, guanine, with radius 1.87 \AA , was placed at the coordinates of a base in the 2nd–6th rows. The electron-transfer rate was calculated using the Marcus form given in eq 2. λ was calculated using eq 6. ΔG was calculated using eqs 7–9, and 11 with ground-state redox potentials ($E_D^{\text{ox}})_{\text{MeCN}, \epsilon_{\text{st}}=37} = 1.25 \text{ eV vs SCE}$,⁴⁶ ($E_A^{\text{red}})_{\text{DMSO}, \epsilon_{\text{st}}=47} = -1.9 \text{ eV vs SCE}$,¹ and acceptor singlet energy $h\nu = 3.4 \text{ eV}$.¹ Correction of E_A^{red} to $\epsilon_{\text{st}} = 37$ is 0.02 eV , within the error of the original value. The results of our calculations with these ΔG values are not affected by the fact that we chose a classical rate constant rather than a quantum mechanical rate constant.^{47,48} Calculations were also performed for larger donor/acceptor radii of 2.58 and 2.95 \AA for guanine and stilbene, respectively, calculated assuming 4.5 \AA^3 per atom. To avoid donor/acceptor overlap for the large radii, the shortest donor/acceptor distance was ignored.

The experimental data, shown in Figure 7, can be fit well with a simple exponential model of $k(r)$ (eq 1) using $\beta_e = 0.64$

$\pm 0.1 \text{ \AA}^{-1}$. As shown in eq 1, this fit does not include consideration of the distance dependences of the reorganization energy or the free energy change. The parameter β_e in some sense models all three contributions to the distance dependence of electron transfer, that is, the distance dependence of the electronic interaction and the distance dependences of the reorganization energy or the free energy change.

To include all three contributions to the distance dependence explicitly, calculations with the Marcus distance-dependent transfer rate (eq 2) used with the heterogeneous DNA model were performed. The results show a faster transfer rate at the shortest donor/acceptor separation, producing a deviation from the apparently exponential distance dependence of the data. The calculation of a faster transfer rate than the data also occurred when the Marcus homogeneous model was used for the calculations. However, the experimental error is greatest for the first data point because of insufficient time resolution; the reported value may be a lower limit for the rate at the shortest distance.⁴⁵ Therefore, the calculations were only compared to data for which the donor/acceptor molecules had at least one intervening base pair.

Without the 1st experimental point, it was possible to reproduce the data. However, a physically implausible value of $\beta = 0.08 \text{ \AA}^{-1}$ was required to obtain a slope of -0.64 \AA^{-1} from the calculations (see Figure 7). Calculations were insensitive to whether the bases in the 1st row had hydrocarbon properties or whether they were removed and filled in with water. They were also insensitive to whether the smaller or larger donor/acceptor radii were used.

Calculations with $\beta = 0.0 \text{ \AA}^{-1}$ are shown as triangles in Figure 7 and illustrate the contribution of activation energy to the distance dependence of the rate constant (see eq 2). These results show that *if the Marcus rate constant and reorganization energy calculations apply to this experiment*, essentially all of the distance dependence of the rate constant is included in the distance dependence of the activation energy and that the electronic coupling contribution has almost no distance dependence. The very small β , which implies little distance dependence in the electronic coupling, is not an artifact of the heterogeneous model. If a Marcus rate constant (eq 2) is calculated for continuum solvents with a range of dielectric constants, then $\beta = 0.12, 0.07,$ and 0.06 \AA^{-1} are obtained for solvents with the dielectric properties of pyridine, propanol, and water, respectively. Pyridine has the lowest dielectric constant of these, with $\epsilon_{\text{st}} = 12.4$. Modeling the entire DNA–water system with a dielectric constant this low seems unreasonable given that the stilbenedicarboxamide bridge is exposed directly to water, and $\epsilon_{\text{st, effective}} = 20$ in the minor groove of DNA.⁴¹ The important feature of the calculations is that the distance dependence is dominated by the distance dependence of the reorganization energy and the free energy change regardless of whether the inhomogeneous model or the homogeneous Marcus model is used.

Another physically unreasonable aspect of the calculation is the value obtained for the electronic coupling at contact, J_0 . Even if the first data point is not used, a J_0 value of $500\,000 \text{ cm}^{-1}$ is required to fit the distance dependent data. The calculated rate at contact is an unrealistic 1 fs^{-1} . The values obtained for β and J_0 demonstrate that the experimental system is not behaving in accord with the expectations based the Marcus theory of the distance dependent rate constant.

Lewis et al. have performed additional experiments on systems similar to the ones discussed above.⁴⁸ In their new paper, the transfer rate was measured at two distances in many

different DNA hairpins characterized by different driving forces. A number of assumptions are made in the data analysis, including that the electronic coupling is the same for a variety of distinctly different donor/acceptor pairs and that the same electronic coupling would occur for forward and back electron transfer. Using these assumptions, the reorganization energy at the two distances and a value for β were calculated from the data. The calculations yield $\beta = 0.77 \text{ \AA}^{-1}$, which is more in line with expected values of β .

However, the values obtained for the solvent contribution to the reorganization energy, λ_o are 0.23 and 0.27 eV with 0 and 2 intervening base pairs ($\sim 7 \text{ \AA}$ distance change). These values are much lower than those expected from a Marcus model, and have virtually no distance dependence. The small values of λ_o and the lack of distance dependence are although one of the chromophores is exposed to water. The Marcus form of the solvent reorganization energy, whether it is used in the inhomogeneous model presented here or in the Marcus continuum model, predicts a strong distance dependence for the significant change in distance of 7 \AA . Calculations were performed in which the dielectric constant of the water surrounding the DNA was reduced to 20 and even 10. The results were very similar and not in accord with the results of Lewis et al. Calculations were also performed using the quantum mechanical form of the rate constant⁴⁷ employed by Lewis et al. in their data analysis.⁴⁸ This form still employs the Marcus reorganization energy. The quantum mechanical rate constant with the calculated Marcus form of the reorganization energy is incompatible with the data in the same way that the classical form is.

The calculations using the inhomogeneous electron-transfer model for DNA input the Marcus form of the reorganization energy. Comparison to the distance dependent data of Lewis et al.¹ yield values of β and J_o that are unphysical for a single step Marcus-like electron transfer. The calculations show that virtually all of the distance dependence is in the activation energy, that is, the combined solvent reorganization energy and the free energy change. The recent results of Lewis et al.⁴⁸ yield reasonable values of β and J_o , but give a magnitude and a distance dependence of the solvent reorganization energy that are not consistent with Marcus form of the reorganization energy. The combination of the results suggest that electron transfer in the systems studied by Lewis et al. are not properly described by the distance dependent Marcus rate constant.

The experimental system of Lewis et al. seems to behave in a significantly different manner than the Brun-Harriman system. The heterogeneous model presented here is approximate. Some error comes from lack of precise knowledge of the DNA base/backbone dielectric constants or the donor/acceptor hard sphere radii. The polyelectrolyte nature of DNA has not been included in the model. However, in other systems, it has been shown that electrolyte contributions to electrostatic potentials are minor compared to overall polar solvent effects.⁴⁹ Although the details of the heterogeneous DNA model affect the values calculated, the major qualitative difference between rates calculated with the heterogeneous DNA model and the simple exponential model is due to the distance dependence of λ and ΔG , rather than to the exact nature of the heterogeneous model. Rates calculated using the heterogeneous DNA model are similar to Marcus continuum rates for the same donor/acceptor with moderate solvent polarities. For the distance dependence measured by Lewis et al. to approximately reflect the distance dependence of the electronic interactions, errors in the heterogeneous model or the lack of applicability of the homogeneous Marcus model would have to almost completely remove the

calculated distance dependence of λ and ΔG . There is no reason to assume that λ and ΔG have essentially no distance dependence in the experimental system under consideration.

IV. Concluding Remarks

This work has employed an approximate model to demonstrate the importance of including the distance dependence of the reorganization energy and the free energy change in calculation of the rate of electron transfer in DNA. The model includes the heterogeneous nature of the dielectric environment. Rates calculated assuming a DNA-like heterogeneous dielectric environment are similar in shape to rates calculated assuming a continuum dielectric model. However, it not possible to predict which continuum dielectric properties can be used to approximate the heterogeneous DNA structure for a given set of molecular charges, sizes, and energy levels. Including distance-dependent solvent reorganization energy and free energy of transfer is necessary to obtain an understanding of the distance dependence of the electronic coupling. Rates calculated with distance-dependent λ and ΔG are very different from simple exponential rates calculated with the same β (distance dependence of the electronic coupling). Comparison of the detailed theory to experimental data of Lewis et al.¹ strongly suggests that the Marcus form of the distance dependence of the transfer rate constant including the Marcus reorganization energy is not consistent with the data.

This paper presents a first step toward more realistically modeling the heterogeneous nature of duplex DNA and its effects on the distance dependence of electron transfer in DNA. Despite its limitations, the model presented includes many of the important features necessary for a proper description of electron transfer in DNA. The calculations presented here set the stage for future considerations of all of the factors that give rise to the distance dependence of electron transfer in DNA.

Acknowledgment. We would like to thank Professors Frederick D. Lewis and Michael R. Wasielewski, Department of Chemistry, Northwestern University, for providing preprints of their work. We would like to thank Dr. Marshall Newton, Brookhaven National Laboratory, for very helpful discussions concerning this work. We would also like to thank Florence Laine for developing a system of converting X-ray crystallographic coordinates to our multisphere model and for performing some of the preliminary calculations. This research was supported by the Department of Energy, Office of Basic Energy Sciences (Grant DE-FG03-84ER13251).

Appendix A

The integrations in eqs 4, 6, 10, and 11 can be calculated analytically when all space is comprised of a solvent and spherical regions with different dielectric properties whose surfaces do not intersect with each other or with the donor/acceptor sphere surfaces.^{18,26} In other cases, the integrals must be evaluated numerically. If one of the spherical regions is completely contained within another, the contribution of the larger sphere over the volume of the smaller sphere must be subtracted in the same manner that solvent contributions are subtracted over the volumes of the other spheres in eqs 6, 10 and 11, and the integrations can be carried out analytically. Calculations can also be performed analytically for the case in which the donor/acceptor spheres are both contained within third sphere, following the previously published example of electron transfer in micelles.¹⁸

In all of these cases, the following analytical solutions to the integrals can be used:^{18,26}

$$\begin{aligned} \frac{1}{4\pi} \int_{\infty-\nu_D-\nu_A}^{\nu_D} (d\mathbf{E}_D \pm a\mathbf{E}_A)^2 dV &= \frac{d^2}{4\pi} \int_{\infty-\nu_D}^{\nu_D} \mathbf{E}_D^2 dV + \\ \frac{a^2}{4\pi} \int_{\infty-\nu_A}^{\nu_A} \mathbf{E}_A^2 dV \pm \frac{da}{2\pi} \int_{\infty-\nu_D-\nu_A}^{\nu_D} \mathbf{E}_D \mathbf{E}_A dV &- \frac{d^2}{4\pi} \int_{\nu_A}^{\nu_D} \mathbf{E}_D^2 dV - \\ \frac{a^2}{4\pi} \int_{\nu_D}^{\nu_A} \mathbf{E}_A^2 dV &= \frac{d^2}{a_D} + \frac{a^2}{a_A} \pm \frac{2da}{r} - d^2 f(r, a_A) - a^2 f(r, a_D) \end{aligned} \quad (\text{A1})$$

$$\begin{aligned} \frac{1}{4\pi} \int_{\nu_q} (d\mathbf{E}_D \pm a\mathbf{E}_A)^2 dV &= \\ \frac{d^2}{4\pi} \int_{\nu_q} \mathbf{E}_D^2 dV + \frac{a^2}{4\pi} \int_{\nu_q} \mathbf{E}_A^2 dV \pm \frac{da}{2\pi} \int_{\nu_q} \mathbf{E}_D \mathbf{E}_A dV &= \\ d^2 f(R_{Dq}, a_q) + a^2 f(R_{Aq}, a_q) \pm da L(\rho(a_q), \gamma_q) \end{aligned} \quad (\text{A2})$$

where d and a are constants. ν_q and a_q denote the volume and radius, respectively, of a spherical dielectric region q or a donor/acceptor sphere D/A . r is the donor/acceptor center-to-center separation distance. $\rho(a_q) = a_q/\sqrt{R_{Dq}R_{Aq}}$, where $R_{Dq/Aq}$ are the center-to-center distances from the donor/acceptor to a spherical region q . γ_q is the angle between lines drawn between the centers of the donor/acceptor molecules and the center of the sphere q ($\cos \gamma_q = (R_{Dq}^2 + R_{Aq}^2 - r^2)/(2R_{Dq}R_{Aq})$). The first three terms in eq A1 are the Marcus solvent reorganization energy terms for a continuum solvent. f are correction factors for donor/acceptor volumes:⁵⁰

$$f(r, a_q) = \frac{a_q}{2|r^2 - a_q^2|} - \frac{r - a_q}{4r|r - a_q|} \ln \frac{r + a_q}{|r - a_q|} \quad (\text{A3})$$

Finally,

$$L(\rho(a_q), \gamma_q) = \frac{1}{\sqrt{R_{Dq}R_{Aq}}} \sum_{n=0}^{\infty} \left(1 \mp \frac{1}{2n+1} \right) \rho^{\pm(2n+1)} P_n(\cos \gamma) \quad (\text{A4})$$

where $P_n(x)$ denote Legendre polynomials. The upper sign corresponds to $\rho(a_q) < 1$, when the donor/acceptor are outside the spherical region q . The lower sign applies when the donor/acceptor spheres are both contained within region q .

References and Notes

- Lewis, F. D.; Wu, T.; Zhang, Y.; Letsinger, R. L.; Greenfield, S. R.; Wasielewski, M. R. *Science* **1997**, *277*, 673.
- Brun, A. M.; Harriman, A. *J. Am. Chem. Soc.* **1992**, *114*, 3656.
- Lewis, F. D.; Wu, T. F.; Liu, X. Y.; Letsinger, R. L.; Greenfield, S. R.; Miller, S. E.; Wasielewski, M. R. *J. Am. Chem. Soc.* **2000**, *122*, 2889.
- Dandliker, P. J.; Holmlin, R. E.; Barton, J. K. *Science* **1997**, *275*, 1465.
- Dandliker, P. J.; Nunez, M. E.; Barton, J. K. *Biochemistry* **1998**, *37*, 6491.
- Holmlin, R. E.; Dandliker, P. J.; Barton, J. K. *Angew. Chem., Int. Ed. Engl.* **1997**, *36*, 2715.
- Kelley, S. O.; Holmlin, R. E.; Stemp, E. D. A.; Barton, J. K. *J. Am. Chem. Soc.* **1997**, *119*, 9861.
- Kelley, S. O.; Barton, J. K. *Chem. Biol.* **1998**, *5*, 413.
- Kelley, S. O.; Barton, J. K. *Science* **1999**, *283*, 375.
- Giese, B.; Wessely, S.; Spormann, M.; Lindemann, U.; Meggers, E.; Michel-Beyerle, M. E. *Angew. Chem., Int. Ed. Engl.* **1999**, *38*, 996.
- Meggers, E.; Michel-Beyerle, M. E.; Giese, B. *J. Am. Chem. Soc.* **1998**, *120*, 12950.
- Fukui, K.; Tanaka, K. *Angew. Chem., Int. Ed. Engl.* **1998**, *37*, 158.
- Brun, A. M.; Harriman, A. *J. Am. Chem. Soc.* **1994**, *116*, 10383.
- Krider, E. S.; Meade, T. J. *J. Biol. Inorg. Chem.* **1998**, *3*, 222.
- Jortner, J.; Bixon, M.; Langenbacher, T.; Michel-Beyerle, M. E. *Proc. Natl. Acad. Sci. U.S.A.* **1998**, *95*, 12759.
- Felts, A. K.; Pollard, W. T.; Friesner, R. A. *J. Phys. Chem.* **1995**, *99*, 2929.
- Chen, E. S.; Chen, E. C. M. *Bioelectrochem.* **1998**, *46*, 15.
- Tavernier, H. L.; Barzykin, A. V.; Tachiya, M.; Fayer, M. D. *J. Phys. Chem. B* **1998**, *102*, 6078.
- Marcus, R. A. *J. Chem. Phys.* **1956**, *24*, 966.
- Marcus, R. A. *J. Chem. Phys.* **1956**, *24*, 979.
- Rehm, D.; Weller, A. *Isr. J. Chem.* **1970**, *8*, 259.
- Swallen, S. F.; Weidemaier, K.; Tavernier, H. L.; Fayer, M. D. *J. Phys. Chem.* **1996**, *100*, 8106.
- Marcus, R. A. *Annu. Rev. Phys. Chem.* **1964**, *15*, 155.
- Bolton, J. R.; Archer, M. D. Basic Electron-Transfer Theory. In *Electron Transfer in Inorganic, Organic, and Biological Systems*; Bolton, J. R., Mataga, N., McLendon, G., Eds.; The American Chemical Society: Washington, 1991; pp 7–23.
- Purcell, K. F.; Blaise, B. Theory of Electron-Transfer Reactions. In *Photoinduced Electron Transfer: Part A. Conceptual Basis*; Fox, M. A., Chanon, M., Eds.; Elsevier: New York, 1988; pp 123–160.
- Barzykin, A. V.; Tachiya, M. *Chem. Phys. Lett.* **1998**, *285*, 150.
- Marcus, R. A.; Sutin, N. *Biochim. Biophys. Acta* **1985**, *811*, 265.
- Tachiya, M. *Chem. Phys. Lett.* **1994**, *230*, 491.
- Weller, A. *Z. Phys. Chem. NF* **1982**, *133*, 93.
- Nunn, C. M.; Neidle, S. *J. Med. Chem.* **1995**, *38*, 2317.
- Mazur, J.; Jernigan, R. L. *Biopolymers* **1991**, *31*, 1615.
- Kremer, F.; Huwe, A.; Arndt, M.; Behrens, P.; Schwieger, W. J. *Phys.: Condens. Matter* **1999**, *11*, A175.
- Friedman, R. A.; Honig, B. *Biopolymers* **1992**, *32*, 145.
- Simonson, T.; Perahia, D. *Proc. Natl. Acad. Sci. U.S.A.* **1995**, *92*, 1082.
- Simonson, T. *Int. J. Quantum Chem.* **1999**, *73*, 45.
- Sutin, N. Nuclear and Electronic Factors in Electron Transfer: Distance Dependence of Electron-Transfer Rates. In *Electron Transfer in Inorganic, Organic, and Biological Systems*; Bolton, J. R., Mataga, N., McLendon, G., Eds.; The American Chemical Society: Washington, 1991; pp 25–43.
- Hale, J. M. The Rates of Reactions Involving Only Electron Transfer, at Metal Electrodes. In *Reactions of Molecules at Electrodes*; Hush, N. S., Ed.; Wiley-Interscience: New York, 1971; pp 229–257.
- Liu, J. Y.; Bolton, J. R. *J. Phys. Chem.* **1992**, *96*, 1718.
- Markel, F.; Ferris, N. S.; Gould, I. R.; Myers, A. B. *J. Am. Chem. Soc.* **1992**, *114*, 6208.
- Riddick, J. A.; Bunger, W. B. *Organic Solvents: Physical Properties and Methods of Purification*, 3rd ed.; John Wiley & Sons: New York, 1970; Vol. II.
- Jin, R.; Breslauer, K. J. *Proc. Natl. Acad. Sci. U.S.A.* **1988**, *85*, 8939.
- Yonemoto, E. H.; Saupe, G. B.; Schmehl, R. H.; Hubig, S. M.; Riley, R. L.; Iverson, B. L.; Mallouk, T. E. *J. Am. Chem. Soc.* **1994**, *116*, 4786.
- Harriman, A. *Angew. Chem., Int. Ed. Engl.* **1999**, *38*, 945.
- Kumar, K.; Kurnikov, I. V.; Beratan, D. N.; Waldeck, D. H.; Zimmt, M. B. *J. Phys. Chem. A* **1998**, *102*, 5529.
- Lewis, F. D. Private communication.
- Seidel, C. A. M.; Schulz, A.; Sauer, M. H. M. *J. Phys. Chem.* **1996**, *100*, 5541.
- Jortner, J. *J. Chem. Phys.* **1976**, *64*, 4860.
- Lewis, F. D.; Kalgutkar, R. S.; Wu, Y.; Liu, X.; Liu, J.; Hayes, R. T.; Wasielewski, M. R. *J. Am. Chem. Soc.*, submitted for publication.
- Marcus, R. A. Theory and Applications of Electron Transfers at Electrodes and in Solution. In *Special Topics in Electrochemistry*; Rock, P. A., Ed.; Elsevier: Amsterdam, 1977; pp 161–179.
- Kharkats, Y. I. *Electrochimica Acta* **1973**, *9*, 881.